 doi:10.20944/preprints202102.0427.v1

A molecular interpretation of the dynamics of diffusive mass transport of water within a glassy polyetherimide

Andrea Correa[1], Antonio De Nicola[2,*], Giuseppe Scherillo[3], Valerio Loianno[3], Domenico Mallamace[4], Francesco Mallamace[5], Hiroshi Ito[2], Pellegrino Musto[6,*], Giuseppe Mensitieri[3,*].

[1] Department of Chemical Sciences, University of Naples Federico II, Via Cintia, Complesso Monte S. Angelo, 80126 Napoli, Italy

[2] Graduate School of Organic Materials Science, Yamagata University, 4-3-16 Jonan, Yonezawa, Yamagata 992-8510, Japan.

[3] Department of Chemical, Materials and Production Engineering, University of Naples Federico II, Piazzale Tecchio 80, 80125 Naples, Italy

[4] Departments of ChiBioFarAm and MIFT- Section of Industrial Chemistry, University of Messina, CASPE-INSTM, V.le F. Stagno d'Alcontres 31, 98166 Messina, Italy

[5] Department of Nuclear Science and Engineering, Massachusetts Institute of Technology, Cambridge, MA 02139, USA

[6] Institute on Polymers, Composites and Biomaterials, National Research Council of Italy, via Campi Flegrei, 34, Pozzuoli (Naples) 80078, Italy

Abstract

The diffusion process of water molecules within a polyetherimide (PEI) glassy matrix has been analyzed by combining the experimental analysis of water sorption kinetics performed by FTIR spectroscopy with theoretical information gathered from Molecular Dynamics simulations and with the expression of water chemical potential provided by a non-equilibrium lattice fluid model able to describe the thermodynamics of glassy polymers. This approach allowed to construct a convincing description of the diffusion mechanism of water in PEI providing molecular details of the process related to the effects of the cross- and self-hydrogen bondings established in the system on the dynamics of water mass transport.

KEYWORDS: water, polyetherimide, hydrogen bonding, diffusion, molecular dynamics.

Preprints (www.preprints.org) | NOT PEER-REVIEWED | Posted: 19 February 2021 doi:10.20944/preprints202102.0427.v1

1. Introduction

Transport of water in polymeric systems is accompanied by hydrogen bonding self-interaction between water molecules and, frequently, by cross-interactions between water molecules and proton acceptor and proton donor groups present in the polymer backbone as well as self-interactions involving macromolecules. Interactional issues are relevant in a series of technological applications of polymers, as is the case of membranes for separation of gaseous and vapor mixtures, polymeric films with barrier properties to water vapor, environmental durability of polymer matrices for composites and humidity sensor applications [1-6]. Prompted by this motivation, several studies have been carried out to address the fundamental issue of understanding sorption thermodynamics of water in high performance glassy polymers. In particular, in a series of previous contributions by our group,[7] [8] [9] [10-11] the thermodynamics of polyimides-water systems was investigated, combining experimental approaches based on vibrational spectroscopy and gravimetric analysis with theoretical approaches based on Quantum Chemistry – Normal Coordinate Analysis (QC-NCA) and on an Equation of State (EoS) statistical thermodynamics theory based on a compressible lattice fluid model. To this aim, we adopted the Non Random Hydrogen Bonding theory (NRHB), developed by Panayiotou et al., [12-13] that accounts for specific interactions as well as for non random distribution of contacts between the lattice sites occupied by the components of the mixture and the empty sites. This theoretical framework, originally developed to address the case of sorption thermodynamics of low molecular weight compounds in rubbery polymers, has been then extended to deal with the case of glassy polymers [9]. To this purpose the non-equilibrium nature of glassy systems was specifically taken into account by introducing the Non-Random Hydrogen Bonding - Non equilibrium Theory for Glassy Polymers – (NRHB- NETGP).

More recently [10], we have analyzed the sorption thermodynamics of PEI-water system. To perform a comprehensive analysis of this interacting system, the information gathered from gravimetric and vibrational spectroscopy experimental investigations were combined not only with QC-NCA and NRHB-NETGP theoretical approaches but also by exploiting the wealth of information at the molecular level provided by Molecular Dynamics (MD) simulation. In fact, MD simulation delivered relevant evidences that were used to confirm and complete the physical picture emerging from the outcomes of vibrational spectroscopy and of macroscopic thermodynamics modeling. The results of this multidisciplinary approach allowed to determine a comprehensive physical picture of the hydrogen bonding which establish within the system. The outcomes of MD simulations and of gravimetric and spectroscopic experimental analyses were in good qualitative and quantitative

Preprints (www.preprints.org) | NOT PEER-REVIEWED | Posted: 19 February 2021 doi:10.20944/preprints202102.0427.v1

agreement with the results of statistical thermodynamics modelling (NRHB- NETGP). Notably, the amount of the different types of self- and cross-interactions were determined as a function of total concentration of water.

The present contribution, starting from the relevant results obtained in the previous analysis focused on equilibrium thermodynamics of PEI-water system, is addressed to the exploration of the dynamics of mass transport of water in glassy PEI. After a short background section summarizing the most relevant results emerging from the equilibrium analysis the new results on the dynamics of transport of water molecules within PEI matrix and on lifetimes of the different types of hydrogen bonding are presented. A molecular insight into diffusion mechanisms of water in PEI is provided by MD simulations, determining theoretical values for water *intra-diffusion* coefficient in PEI in the limit of vanishingly small concentrations. These values were found to be consistent with values of *mutual* diffusivity determined from time-resolved FTIR spectroscopy, in the same limit of small water concentration. In addition, the time-dependent behavior of HB bonds is presented, focusing on the mean bond lifetime that is the most accessible property reflecting this kind of behavior.

Preprints (www.preprints.org) | NOT PEER-REVIEWED | Posted: 19 February 2021 doi:10.20944/preprints202102.0427.v1

2. Background

2.1 *Relevant results on equilibrium thermodynamics of PEI-water system*

Vibrational spectroscopy provided the molecular level information onto which the NRHB-NETGP thermodynamic modelling is rooted. In particular, we considered the normal modes of the water molecule in the ν(OH) frequency range (3800−3200 cm^{-1}), which were isolated by Difference Spectroscopy (DS), upon elimination of the polymer matrix interference. [11] Using this approach, it was also possible to determine the evolution with sorption time of the ν(OH) profile. The complex, partially resolved pattern, suggesting the occurrence of more than one species of penetrant, was interpreted with the aid of two-dimensional correlation analysis. [10]. It was concluded that two couples of signals are present, each belonging to a distinct water species. In particular, the sharp peaks at 3655–3562 cm^{-1} were assigned to isolated water molecules interacting via H-bonding with the PEI backbone (cross-associated or *first-shell* water molecules). The first shell adsorbate was found to have a 2:1 stoichiometry, with a single water molecule bridging two carbonyls (i.e. –C=O···H–O–H···O=C–). A second doublet at 3611–3486 cm^{-1} was associated with water molecules self-interacting with the first shell species through a single H-bonding (self-associated or *second-shell* water molecules). Analysis of the substrate spectrum revealed that the active sites (proton acceptors) on the polymer backbone are the imide carbonyls, while the involvement of the ether oxygens is negligible, if any.

A schematic diagram representing the two water species identified is reported in Fig. 1

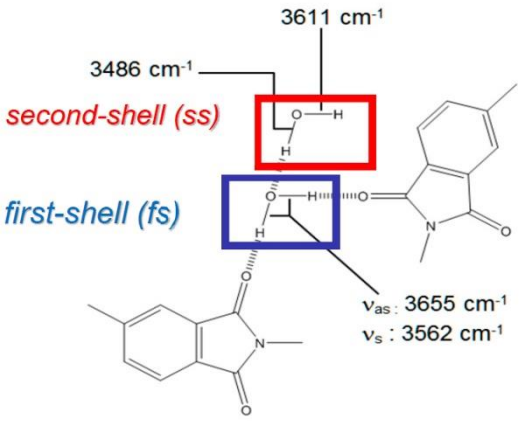

Figure 1. The water species identified spectroscopically, with indication of the signals they produce.

Preprints (www.preprints.org) | NOT PEER-REVIEWED | Posted: 19 February 2021 doi:10.20944/preprints202102.0427.v1

Analysis of the ν(OH) band profile by least-squares curve fitting [10] allowed us to quantify the *ss* and *fs* population. Water species concentrations within the PEI, as determined at sorption equilibrium with water vapour at different pressures and at T = 303.15 K, in units relevant to the thermodynamic analysis, are represented in Fig. 2 as a function of the content of water absorbed in the polymer. In agreement with FTIR analysis MD simulations [10] identified two main different water populations: first shell, *fs*, and second shell, *ss*, water molecules. *Fs* water molecules interact directly with PEI carbonyl groups, while the *ss* water population is consisting of water molecules interacting with *fs* water molecules. The results of MD simulations highlighted how the *fs* water population mainly consists of water molecules bridging two consecutive intrachain carbonyls of the same PEI chain. Some interchain water bridges were also identified but they are reported to be present in a fraction from 0 to around 0.3 of all bridged water molecules, going from the lower water concentration to the higher water concentration system. Moreover, no significant involvement of PEI ether groups in hydrogen bond formation emerged from the MD results reported in ref [10].

In the same contribution, the thermodynamics of the PEI/water system at sorption equilibrium with a water vapor phase at prescribed pressure values has been analyzed on the basis of the NRHB-NETGP model for mixtures [10]. As anticipated, the NRHB- NETGP approach is a lattice fluid theory able to account for non-equilibrium nature of glassy polymers, for the presence of self- and cross-hydrogen bonding and for non-random mixing of the two components. The reader is referred to the relevant literature [9] [11] for the relevant equations of the NETGP-NRHB model. It suffices here to remind that the application of this theory provides a quantitative prediction on the type and number of hydrogen bonds formed at equilibrium within the system, once that the model has been used to fit experimental sorption isotherms of a penetrant within a polymer. In particular, the results of the application of NETGP-NRHB theory to the PEI/H_2O system, evidenced that the predictions on HB formation at equilibrium agree very well with the experimental results obtained by in situ infrared spectroscopy and with the theoretical results obtained by MD simulations.[10]. This is evident in Fig. 2 where this comparison is reported with reference to the HB interactions actually established in the system, i.e. water self-interactions (indicated by '11' subscript) and water – PEI (carbonyl group) cross-interactions (indicated by '12' subscript).

Preprints (www.preprints.org) | NOT PEER-REVIEWED | Posted: 19 February 2021 doi:10.20944/preprints202102.0427.v1

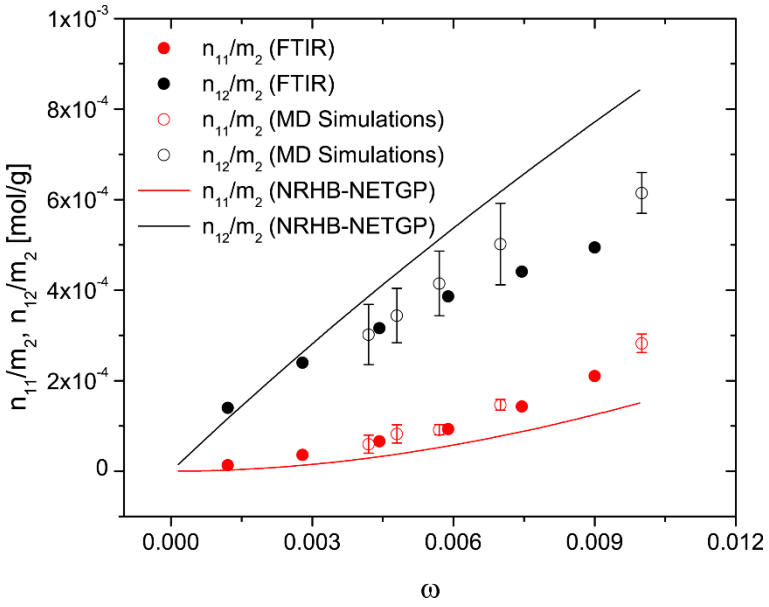

Figure 2. Comparison of the predictions of the NETGP-NRHB model for the amount of self and cross-HBs with the outcomes of FTIR spectroscopy and of MD simulations. Reprinted with permission from reference [10]. Copyright (2017) American Chemical Society.

On this basis, it was concluded that the NRHB-NETGP theory provides a reliable expression of the chemical potential of H_2O in glassy PEI. This expression will be used in the present contribution to evaluate the thermodynamic factor that appears in the theoretical expression of PEI/H_2O *mutual* diffusivity, as detailed in the following section (see eq. (12)).

2.2 *Mutual*- vs. *intra*-diffusion coefficients

Diffusive mass transport of small molecules in polymers is a multifaceted phenomenon whose description, in the most complex cases, involve concurrently mass, momentum and energy balances with the introduction of thermodynamically consistent constitutive equations for the different types of flux implicated and for the relevant material properties. As a starting point, it is important to provide a description of the basic approaches used to express the mass flux of a component 'i' in a mixture. We will address here the general case, although our final goal is to deal with mass transport in an isotropic system formed by a low molecular weight compound (penetrant) dissolved within a polymer matrix.

Preprints (www.preprints.org) | NOT PEER-REVIEWED | Posted: 19 February 2021 doi:10.20944/preprints202102.0427.v1

In a binary mixture, the total mass flux of component *i*, $\underline{n}_i$, referred to a lab fixed frame of reference is expressed as:

$$\underline{n}_i = \rho_i \underline{u}_i = \underline{j}_i^M + \rho_i \underline{u}^M \tag{1a}$$

or, equivalently, as:

$$\underline{n}_i = \rho_i \underline{u}_i = \underline{j}_i^V + \rho_i \underline{u}^V \tag{1b}$$

where

$$\underline{u}^M \equiv \omega_1 \underline{u}_1 + \omega_2 \underline{u}_2 \tag{2a}$$

is the mass average mixture velocity referred to a lab fixed frame of reference while

$$\underline{u}^V \equiv c_1 \overline{\upsilon}_1 \underline{u}_1 + c_2 \overline{\upsilon}_2 \underline{u}_2 \tag{2b}$$

is the volume average mixture velocity referred, again, to a lab fixed frame of reference. In the previous equations c_i, ρ_i, ω_i and $\overline{\upsilon}_i$ represent, respectively, the molar concentration of component *i*, the mass of component *i* per volume of mixture, the mass fraction of component *i* and the partial molar volume of component *i*. The symbol $\underline{u}_i$ represents the velocity of molecules of component *i*, referred to a lab fixed frame of reference. In the present context, we deal with the specific case of penetrant-polymer mixtures and we will refer to the penetrant with subscript 1 and to the polymer with the subscript 2. From the previous equations (1a,b) it is readily derived that:

$$\underline{j}_i^M \equiv \rho_i \cdot (\underline{u}_i - \underline{u}^M) \tag{3a}$$

$$\underline{j}_i^V \equiv c_i \cdot (\underline{u}_i - \underline{u}^V) \tag{3b}$$

Eqs. (3a) and (3b) define, respectively, the diffusive mass flux of component *i* relative to the weight average velocity of the mixture, $\underline{j}_i^M$, and the diffusive molar flux of component *i* relative to the volume average velocity of the mixture, $\underline{j}_i^V$. If the contributions to mass flux determined by a gradient of temperature, a gradient of pressure and by the difference of the body forces acting on unit of mass of each component can be neglected, the following constitutive equation holds for $\underline{j}_i^M$ [14]:

Preprints (www.preprints.org) | NOT PEER-REVIEWED | Posted: 19 February 2021 doi:10.20944/preprints202102.0427.v1

$$\underline{j}_i^M = -D_{12}\rho\underline{\nabla}\omega_i \tag{4}$$

where ρ is the density of the mixture. In the case of constant density, equation (4) takes the classical form of the so-called Fick's first law [14] :

$$\underline{j}_i^M = -D_{12}\underline{\nabla}\rho_i \tag{5}$$

where D_{12} is the *mutual* diffusivity of the '12' system. It is worth noting that, since

$$\sum_i \underline{j}_i^M = 1 \tag{6}$$

and

$$\underline{\nabla}\omega_1 = -\underline{\nabla}\omega_2 \tag{7}$$

a single *mutual-diffusion* coefficient D_{12}, is defined intrinsically by equation (4) for both components. In fact, as we will see in the following, this coefficient is a property of the binary system and is a function of temperature and concentration.

Considering the specific case of isothermal diffusion of water in an unconstrained film of PEI, it is noted that, at the investigated conditions (T=303.15 K, range of relative pressure of water vapor, p/p_0 = 0 ÷ 0.6), the weight fraction of water within the polymer is always lower than 0.01. This implies that no relevant stresses develop as consequence of water sorption. The low amount of penetrant absorbed combined with the absence of polymer swelling allows also the assumption of a constant mixture density. In addition, the bulk velocity of the polymer/water mixture can be considered to be negligible (i.e. $\underline{u}^M \cong 0$; $\underline{u}^V \cong 0$), in view of the low intrinsic mobility of polymer (i.e. $\underline{u}_2 \cong 0$), that is the largely prevailing component. Moreover, the eq (4) can be taken as constitutive expression of the diffusive mass flux since, in the case at hand, other driving forces beside the composition gradient can be ruled out. In fact, i) the driving force related to the difference of the body forces acting per unit of mass of each component is equal to zero since in this case they are only associated to the gravitational field; ii) the driving force related to the gradient of temperature is zero in view of the isotheral condition; iii) the driving force related to the gradient of pressure is zero in view of the uniformity of the state of stress. Finally, it is worth noting that the transport of fluids in polymers is slow enough to assure that also the inertial contributions can be neglected. Therefore:

Preprints (www.preprints.org) | NOT PEER-REVIEWED | Posted: 19 February 2021 doi:10.20944/preprints202102.0427.v1

$$\underline{n}_i \cong \underline{j}_i^M \cong \underline{j}_i^M = -D_{12}\nabla\rho_i \tag{8}$$

In such a case the 1-D differential mass balance on component 'I' reads [14]:

$$\frac{\partial\rho_i}{\partial t} = -\frac{\partial n_i}{\partial x} = -\frac{\partial}{\partial x}\left(-D_{12}\frac{\partial\rho_i}{\partial x}\right) \tag{9}$$

where *x* is a lab fixed coordinate. Eq. (9), in the case of D_{12} independent of composition, takes the form of the so-called Fick's second law [15]:

$$\frac{\partial\rho_i}{\partial t} = D_{12}\frac{\partial^2\rho_i}{\partial x^2} \tag{10}$$

Under the same hypotheses and based upon a well-established statistical mechanics framework Bearman [16] developed a constitutive equation for $\underline{j}_i^V$ in case of a mono-dimensional binary diffusive problem. In this approach it is assumed that, after a chemical potential gradient is established within the binary mixture (due to a concentration gradient), the system attains a local quasi-stationary regime in which the driving force to the diffusion mechanism of a molecule of component *i* (given by its chemical potential gradient) is mechanically balanced by a frictional force deriving from inter-molecular interactions (consisting of both self-interactions, *i-i*, and cross interactions, *i-j* with $j \neq i$). Bearman derived an expression for the frictional forces involving the definition of friction coefficients ζ_{ij} (i,j =1,2) which obey to a reciprocal relationship (i.e., $\zeta_{ij} = \zeta_{ji}$) and, based on this approach, he has also defined a *mutual-diffusion* coefficient, D_{12}^V , analogous to the mass diffusional coefficient D_{12}, such that [16]:

$$j_i^V = -D_{12}^V\frac{dc_i}{dx} \tag{11}$$

where

$$D_{12}^V \equiv \frac{\overline{\upsilon_1}}{\zeta_{12}}RT\left[1+\left(\frac{\partial\ln(f_2)}{\partial\ln(c_2)}\right)_{T,P}\right] = \frac{\overline{\upsilon_2}}{\zeta_{12}}RT\left[1+\left(\frac{\partial\ln(f_1)}{\partial\ln(c_1)}\right)_{T,P}\right] \equiv D_{21}^V \tag{12}$$

Preprints (www.preprints.org) | NOT PEER-REVIEWED | Posted: 19 February 2021 doi:10.20944/preprints202102.0427.v1

In equation (12) f_i represents the activity coefficient of component *i* in the binary system. The equality of the two *mutual* volumetric diffusion coefficients appearing in equations (11) and (12), follows from the Gibbs-Duhem equation and from the definition of volume average velocity.

In view of the simplifying assumptions discussed before, legitimated by the low value of penetrant concentration, it can be derived a relationship involving D_{12}^V and D_{12} for the generic component *i* in the case of mono-dimensional diffusion taking place in direction *x*:

$$M_i D_{12}^V \frac{dc_i}{dx} = D_{12}^V \frac{d\rho_i}{dx} \cong D_{12} \frac{d\rho_i}{dx} \qquad (13a)$$

from which one obtains

$$D_{12}^V \cong D_{12} \qquad (13b)$$

where M_i represents the molecular molar weight of component *i*.

It is useful to introduce now the so called *intra-diffusion* coefficients [17] that represent the intrinsic diffusive mobility of each component in a binary mixture, i.e. in the absence of any driving force for the mass flux (e.g. gradients of chemical potential, temperature, pressure). These coefficients are indicated as, respectively D_1 and D_2. Expressions have been proposed relating the *mutual* diffusivity in a binary mixture, D_{12}, or, similarly, any other type of *mutual-diffusion* coefficient referred to a different frame of reference, to the *intra-diffusion* coefficients of the two components.

On the grounds of statistical mechanics, the three kinds of diffusion coefficients D_{12}, D_1 and D_2 can be expressed in terms of the molecular friction coefficients (in the case at hand penetrant-penetrant, polymer-polymer and penetrant-polymer friction coefficients, respectively denoted by ζ_{11}, ζ_{22} and ζ_{12}) [16]:

$$D = \frac{M_2 \cdot \omega_1 \cdot \hat{V}_2}{N_A^2 \cdot \zeta_{12}} \left(\frac{\partial \mu_1}{\partial \omega_1} \right)_{T,P} \qquad (14a)$$

Preprints (www.preprints.org) | NOT PEER-REVIEWED | Posted: 19 February 2021 doi:10.20944/preprints202102.0427.v1

$$D_1 = \frac{RT}{N_A^2 \cdot \left(\frac{\omega_1 \cdot \zeta_{11}}{M_1} + \frac{\omega_2 \cdot \zeta_{12}}{M_2} \right)} \tag{14b}$$

$$D_2 = \frac{RT}{N_A^2 \cdot \left(\frac{\omega_2 \cdot \zeta_{22}}{M_2} + \frac{\omega_1 \cdot \zeta_{12}}{M_1} \right)} \tag{14c}$$

where N_A is the Avogadro's number.

Actually, *free volume* theories provide independent expressions (see for example [18] [19]) for *intra-diffusion* coefficients, D_1 and D_2, that do not need the knowledge of friction coefficients. However, since three friction coefficients appear in eqs. (14), in general, it is not possible to express D_{12}, only in terms of D_1 and D_2 (i.e. with no friction coefficients), This is, however, possible if special circumstances occur, e.g. if one is able to write a relationship linking the three friction coefficients, or if one considers the limit of trace amount of penetrant, or in the cases where $D_1 >> D_2$. For instance, assuming that ζ_{12} is the geometric mean of ζ_{11} and ζ_{22} [18] [19] or, alternatively, assuming that the ratio between the friction coefficients is constant [16] it is possible to obtain the following relationship:

$$D_{12} \cong D_{12}^V = \frac{\left(D_2 x_1 + D_1 x_2\right)}{RT} \left(\frac{\partial \mu_1}{\partial \ln x_1} \right)_{T,P} = \frac{\left(D_2 x_1 + D_1 x_2\right)}{RT} \left(\frac{\partial \mu_2}{\partial \ln x_2} \right)_{T,P} \tag{15a}$$

where μ_i and x_i represent, respectively, the molar chemical potential and the molar fraction of component i, and P and T represent, respectively, the spatial uniform pressure and temperature of the binary mixture. In the present context $D_1 >> D_2$ and the water molar fraction range is around 0.94-0.97, thus assuring that it is also $D_1 x_2 >> D_2 x_1$. Therefore, the relationship (15a) reduces to an explicit relationship relating the measured *mutual-diffusion* coefficient D_{12} just, to the *intra-diffusion* coefficient of water D_1:

Preprints (www.preprints.org) | NOT PEER-REVIEWED | Posted: 19 February 2021 doi:10.20944/preprints202102.0427.v1

$$D_{12} \cong \frac{D_1}{RT}\left(\frac{\partial \mu_1}{\partial \ln x_1}\right)_{T,P} \qquad (15b)$$

In order to estimate, exclusively on a theoretical basis, the value of D_{12} from eq. (15b) one then need to know the expressions of D_1 and μ_1. In the present investigation, the value of the *intra-diffusion* coefficient has been retrieved from MD simulations of a PEI/H_2O system with uniform concentration, by averaging the statistics of the evolution of the diffusion path with time of each single water molecule. The estimate of μ_1 as a function of concentration has been instead obtained by using the NRHB- NETGP thermodynamic model. The parameters of this for the water/PEI system model are available in a previous publication by our group [10]. The set of equations involved in the calculation of μ_1 according to the NRHB-NETGP has to be solved numerically, so that only an implicit expression for the penetrant molar chemical potential as a function of concentration at a given pressure and temperature is available. Therefore, the derivative of the NRHB- NETGP penetrant molar chemical potential appearing in equation (15b) has been evaluated numerically. In particular, it has been estimated assuming a centered difference finite scheme with a variable concentration step equal to $10^{-6}c_1$. This step has provided an excellent compromise between the accuracy of the approximated numerical scheme adopted and the round-off error deriving from the finite digit arithmetic associated to the calculator used.

The estimates of *mutual* diffusivity, D_{12}, obtained from eq. (15b) for the PEI/H_2O system, based on information provided by MD calculation for D_1 and by NRHB-NETGP model of mixture thermodynamics for μ_1, will be compared with the experimental values obtained independently by in-situ time-resolved infrared spectroscopy.

Finally, it is worth noting that in the limit of a vanishingly small mass fraction of penetrant (water) in the penetrant-polymer systems – and hence in the limit of vanishingly small relative pressure of penetrant (water) vapour – *mutual-diffusion* coefficient, D_{12}, and *intra-diffusion* coefficient of the penetrant, D_1, converge to the same value.[18].

Preprints (www.preprints.org) | NOT PEER-REVIEWED | Posted: 19 February 2021 doi:10.20944/preprints202102.0427.v1

3. Experimental

3.1 Materials

Amorphous PEI with $\overline{M}_n = 1.2 \cdot 10^4\ Da, \overline{M}_w = 3.0 \cdot 10^4\ Da, T_g = 210°C, Density = 1.260\ g/cm^3$ was kindly supplied by Goodfellow Co., PA, USA, in the form of a 50.0 µm thick film. Film thicknesses suitable for FTIR spectroscopy were obtained by dissolving the original product in chloroform (15% wt/wt concentration), followed by solution casting on a tempered glass support. Film thickness in the range 10−40 µm was controlled by using a calibrated Gardner knife to spread the solution over the support. The cast film was dried 1 h at room temperature and 1 h at 80 °C to allow most of the solvent to evaporate, and at 120 °C under vacuum overnight. At the end of the drying protocol, the film was removed from the glass substrate by immersion in distilled water at 80 °C. Milli-Q water was used in all sorption experiments.

3.2 FTIR spectroscopy

Time-resolved FTIR spectra of polymer films exposed to water vapor at a constant relative pressure (p/p_0) were collected in the transmission mode, monitoring the characteristic signature of the penetrant up to the attainment of sorption equilibrium. The sorption experiments were performed in a custom designed, vacuum-tight cell positioned in the sample compartment of the spectrometer. This cell was connected through service lines, to a water reservoir, a turbo-molecular vacuum pump, and pressure transducers. Full details of the experimental setup are reported in ref [20]. Before each sorption measurement, the sample was dried under vacuum overnight at the test temperature in the same measuring apparatus. The FTIR spectrometer was a Spectrum 100 from PerkinElmer (Norwalk, CT), equipped with a Ge/KBr beam splitter and a wide-band deuterated triglycine sulfate (DTGS) detector. Parameters for data collection were set as follows: resolution = 2 cm^{-1}; optical path difference (OPD) velocity, 0.5 cm/s; spectral range, 4000−600 cm^{-1}. A single spectrum collection took 2.0 s to complete under the selected instrumental conditions. Continuous data acquisition was controlled by a dedicated software package for *time-resolved* spectroscopy (*Timebase* from PerkinElmer). The Absorbance spectrum of the penetrant was obtained by use of the single-beam spectrum of the cell containing the dry sample as background. [10]

3.3 MD simulations

Preprints (www.preprints.org) | NOT PEER-REVIEWED | Posted: 19 February 2021 doi:10.20944/preprints202102.0427.v1

3.3.1 Polymer model

The bonded and non-bonded interaction parameters for the full atomistic model of PEI were taken from OPLSAA force-field. [21-23] [24] For non-bonded interactions a cut-off of 1.1 nm was used. Coulomb interactions were treated by generalized reaction field [25] scheme with a dielectric constant ε_{rf} = 5 and a cut-off of 1.1 nm. In order to preserve the system electroneutrality a slight tuning of single point charges was done. Chemical structure of PEI repeating unit is showed in Scheme 1. Each PEI chain used in this work contains 12 repeating units and each chain is terminated by a phenyl group and a hydrogen atom. In PEI/water systems, water molecules were described by the SCP model. [26] Full details on the potentials used to treat non-bonded and bonded interactions and on the values of their parameters are reported in [10] and in the related Supporting information Section.

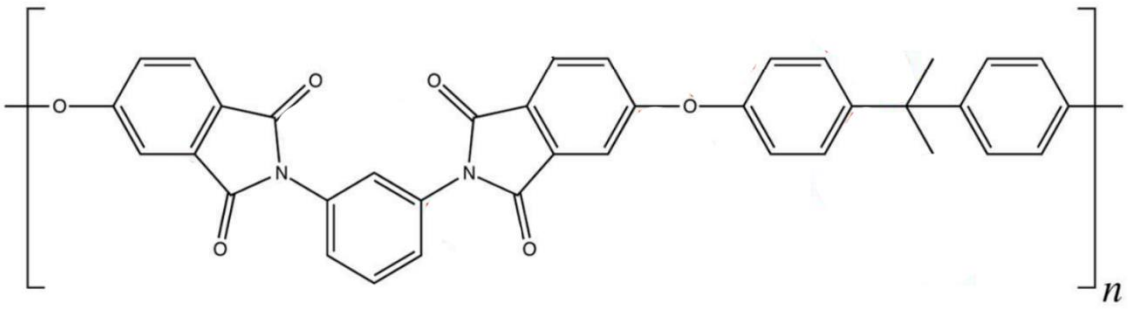

Scheme 1. Chemical structure of PEI repeating unit. For sake of clarity, all hydrogen atoms are omitted. Non bonded interactions over two consecutive bonds are excluded.

3.3.2 Simulation details

Hybrid particle-field molecular dynamics technique (MD-SCF) [27-28] was employed to equilibrate PEI pure amorphous. Simulation runs have been performed, by OCCAM code, [29] in the constant volume and temperature (*NVT*) ensemble, following the same procedure reported by De Nicola et al.,[30] with the temperature fixed at 570 K, controlled by the Andersen thermostat a collision frequency of 7 ps^{-1}, a timestep of 1 fs, and density field density update performed every 0.1 ps. For more details see refs [27-28] [30].

GROMACS package [31] was employed for all atomistic MD simulations. Pure PEI systems were, preliminarily equilibrated for 1 ns in *NVT* ensemble (starting from MD-SCF relaxed structures). All

Preprints (www.preprints.org) | NOT PEER-REVIEWED | Posted: 19 February 2021 doi:10.20944/preprints202102.0427.v1

production runs were performed in the constant pressure and temperature (*NPT*) ensemble, by a timestep of 2 fs. Periodic boundary conditions were applied and, for all systems, a constant number of 27 PEI chains were considered. The temperature was fixed at 303.15 K by Berendsen thermostat (coupling time 0.1 ps). The pressure was kept constant at 1.01325 bar by Berendsen barostat (coupling time 0.1 ps).[32] Table 1 reports composition and simulation details for all simulated systems. For systems I and II five independent MD simulations, with different starting configurations, were performed. For systems with higher water content (i.e., III, IV, V and VI) two independent MD simulations, with different starting configurations, were performed.

Table 1. Systems composition and simulation details.

System	Box (nm3)	W	Water molecules	Total particles	Simulation time (ns)
I	6.31000	-	0	22680	120
II	6.31308	0.0042	86	22938	198
III	6.31358	0.0048	100	22980	200
IV	6.31589	0.0057	120	23040	200
V	6.31980	0.007	150	23130	200
VI	6.32867	0.01	220	23340	240

Preprints (www.preprints.org) | NOT PEER-REVIEWED | Posted: 19 February 2021 doi:10.20944/preprints202102.0427.v1

4. Results and discussion

4.1 Determination of mutual diffusivity of the water-PEI system from vibrational spectroscopy

FTIR spectroscopy has been shown to be a powerful tool to investigate water diffusion in polyimides.[11] For the case at hand the process can be suitably monitored by considering the normal modes of the diffusing molecule in the ν(OH) frequency range (3800 – 3200 cm-1). In fact, difference spectra can be collected in this range as a function of time, providing an accurate evaluation of the sorption/desorption kinetics.

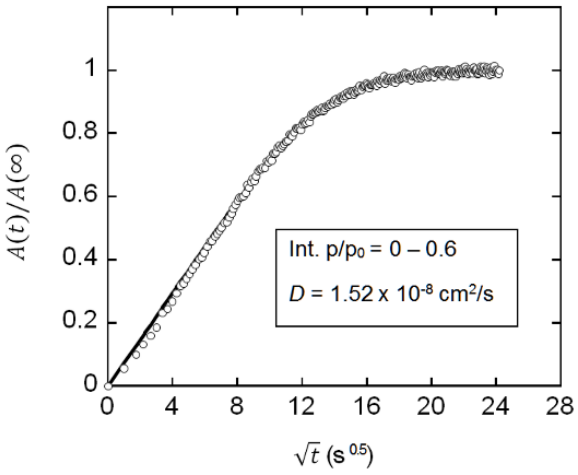

Figure 3. Fick's plot [A(t)/A(∞) vs √t] for the sorption test at p/p_0 = 0.6 at T=303.15 K. The inset displays the time-evolution of the analytical band.

The experimental data were analyzed in terms of the PDE expressing the Fick's second law of diffusion introduced in the background section (see eq. (10)). For the case of a plane sheet exposed to symmetric boundary conditions (i.e., an equal penetrant activity on both sides) the solution of eq. (10) can be expressed as [15, 33]:

$$\frac{A(t)}{A(\infty)} = \frac{M(t)}{M(\infty)} = 1 - \frac{8}{\pi^2}\sum_{m=0}^{\infty}\frac{1}{(2m+1)^2}\cdot\exp\left[\frac{D_{12}(2m+1)^2\pi^2}{L^2}\right] \qquad (16)$$

where *M(t)* and *M(∞)* represent, respectively, the total mass of penetrant absorbed in the polymer sheet at time *t* and at equilibrium, while *A(t)* and *A(∞)* represent, respectively, the absorbance area of the analytical band at time *t* and at equilibrium and *L* is the sample thickness. Equation (16) has

Preprints (www.preprints.org) | NOT PEER-REVIEWED | Posted: 19 February 2021 doi:10.20944/preprints202102.0427.v1

been used to best fit experimental sorption kinetics data using D_{12} as fitting parameter, assumed to be independent on concentration.

In Figure 3 is reported the experimental water sorption kinetics for a step increase of relative pressure of water vapor from 0 to 0.6 ('integral sorption test'). The normalized absorbance of the analytical band, *A(t)/A(∞)*, is plotted as a function of the square root of time (Fick's diagram) for an experiment performed at 303.15 K. The very good fit of the experimental data and the linear dependence of the *A(t)/A(∞)* on the square root of time for ordinate values up to around 0.6, point to the so-called, Fickian behavior of the system [15]. The water-PEI *mutual* diffusivity was found to be 1.52 x 10^{-8} cm^2/s, that is in good agreement with previous literature reports on commercial polyimides.[34]

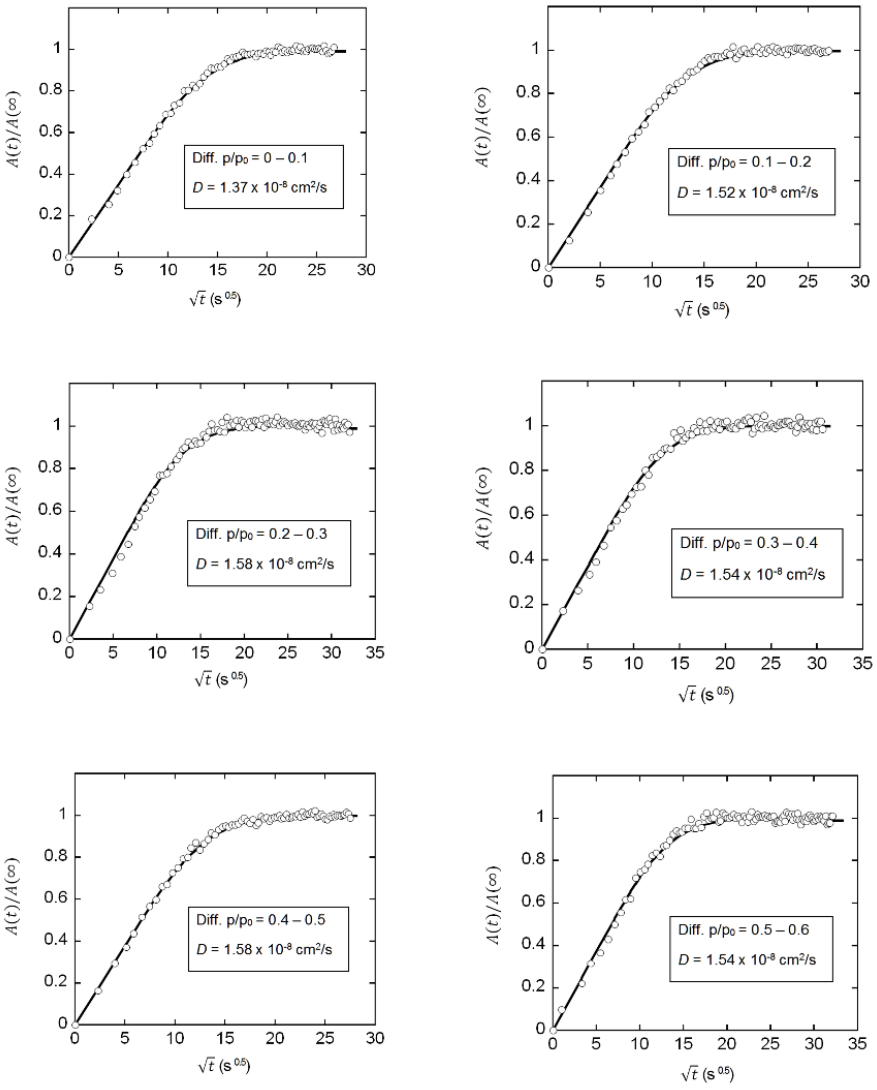

Figure 4. Fick's plots [$A(t)/A(\infty)$ *vs* $\sqrt{t}$] for the 'differential sorption tests' performed in the p/p_0 interval 0 – 0.6.

Preprints (www.preprints.org) | NOT PEER-REVIEWED | Posted: 19 February 2021 doi:10.20944/preprints202102.0427.v1

The kinetic analysis of the diffusion process was also performed in the p/p_0 interval from 0 to 0.6 performing 'differential sorption tests', i.e., increasing stepwise by a 0.1 increment the relative-pressure of H_2O vapor. The related Fick's diagrams are reported in Figure 4. Consistently with the assumption of a constant diffusivity, the D_{12} values obtained from the fitting of kinetics data using eq. (16) are rather independent of concentration [average value: $D_{12} = 1.55 \cdot 10^{-8} \pm 0.03 \cdot 10^{-8}$ cm^2/s]; only at $p/p_0 = 0.1$ the diffusivity is appreciably lower ($D_{12} = 1.37 \cdot 10^{-8} \pm 0.03 \cdot 10^{-8}$ cm^2/s).

The values of water-PEI *mutual* diffusivity coefficients as determined by best fitting the experimental sorption kinetics data using eq. (16) are collectively reported in figure 5.

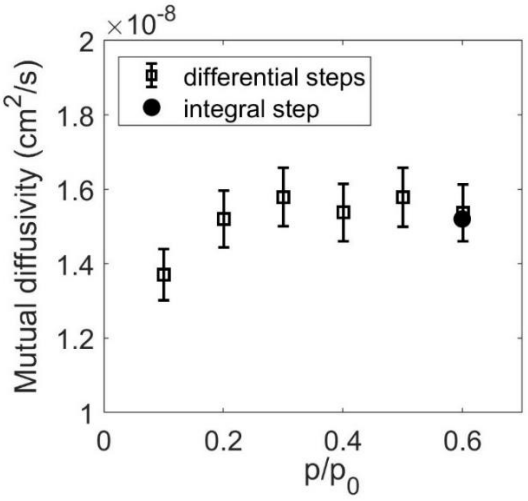

Figure 5. Values of water-PEI *mutual* diffusivity, D_{12}, determined from FTIR spectroscopy reported as a function of relative pressure of H_2O vapor at 303.15 K.

4.2 Molecular dynamics simulations

Before performing simulations of water diffusion within the PEI/water system, relaxation of PEI atomistic model has been obtained to generate a well-equilibrated system of full atomistic polymer melts at 570 K, followed by fast quenching from 570 to 303.15 K, using a MD-SCF approach, as reported in [10]. The obtained configurations, corresponding to 'System I' reported in Table 1, have been used to build up systems at different water concentrations by insertion of water molecules.

Values of *intra-diffusion* coefficient of water have been theoretically calculated on the basis of the mean square displacement as a function of time of each water molecule present within a PEI domain resulting from molecular dynamics simulations at several uniform water concentrations.

Preprints (www.preprints.org) | NOT PEER-REVIEWED | Posted: 19 February 2021 doi:10.20944/preprints202102.0427.v1

The values of *intra-diffusion* coefficient of water as determined from the simulations performed at T = 303.15 K are reported in Fig. 6 as a function of mass fraction of water.

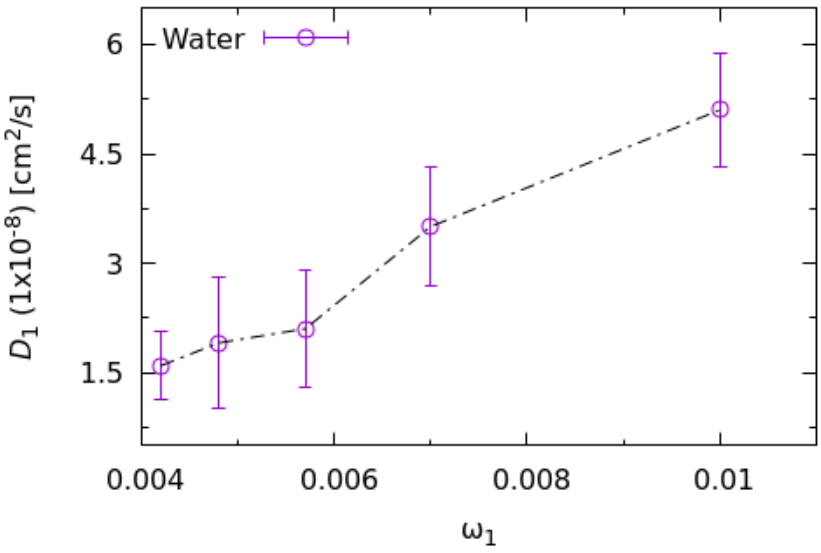

Figure 6. *Intra-diffusion* coefficient of water calculated from mean square displacement of molecular dynamics simulations at different water concentration.

As anticipated, the *intra-diffusion* coefficient represents the absolute intrinsic mobility of a water molecule within the PEI/water mixture in the absence of any gradient of water chemical potential and of any other driving force for mass transport. Conversely, the *mutual-diffusion* coefficient represents water mobility as referred to the mass average velocity of the polymer-water mixture, under the action of a gradient of chemical potential of water and/or of other driving forces. In general, these two coefficients have different values. However, based on reasonable assumptions, it has been already discussed that, in the limit of vanishingly small mass fraction of water in the water-polymer systems - and hence in the limit of vanishingly small relative pressure of water vapour - *mutual diffusion* coefficient and *intra-diffusion* coefficient tend to the same value. Actually, the diffusivity value estimated from FTIR spectroscopy measurements and the *intra-diffusion coefficient* predicted on the basis of MD simulation apparently converge to a common value of about $1.20 \cdot 10^{-8}$ cm^2/s at a vanishingly small water concentration, thus confirming the consistency of MD simulations.

In order to have a qualitative molecular interpretation of the possible molecular nature of different dynamic states of water molecules, as indicated by the FTIR spectra analysis, the behavior

Preprints (www.preprints.org) | NOT PEER-REVIEWED | Posted: 19 February 2021 doi:10.20944/preprints202102.0427.v1

of i*ntra-diffusion* coefficients obtained on the basis of MD simulations, averaging over all simulated water molecules, is decomposed as a distribution. In particular, the distribution of the diffusion coefficient obtained from each water molecule as a histogram for two different water concentration is reported in Figures 7A and 7B. From the Figure 7A it is clear that a tail of faster diffusing water molecules is obtained for the system at higher water concentration as compared to the system at lower concentration (Figure 7B).

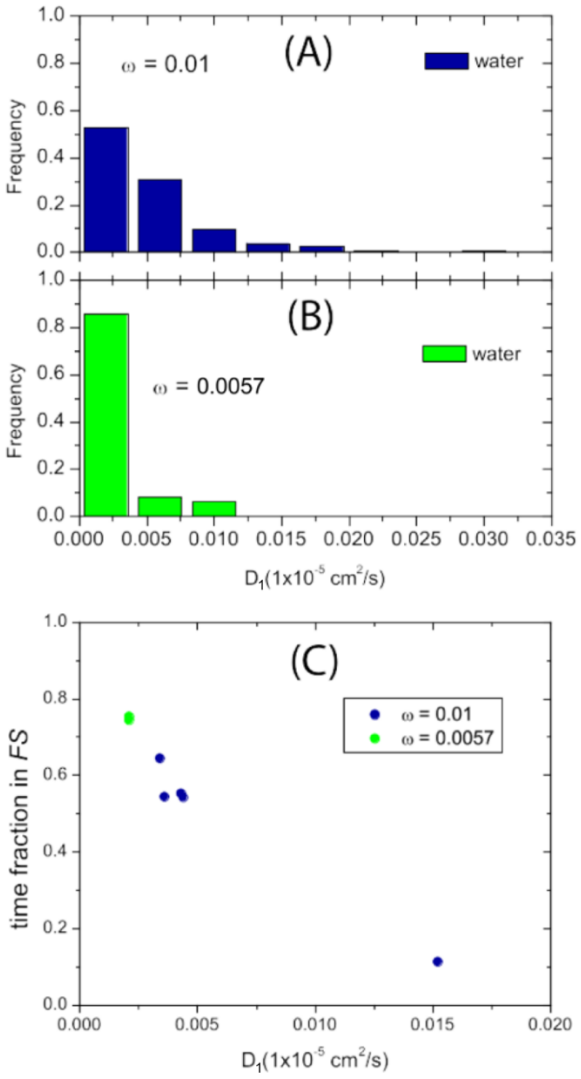

Figure 7. Distribution of self diffusion coefficients of water molecules for two compositions: (A) ω = 0.01 and (B) ω = 0.0057 (C) Distribution of water self diffusion coefficients weighted by the time spent by each water molecule forming hydrogen bonds with acceptor AC1 (only first shell) for both compositions ω = 0.01 (blue points) and ω = 0.0057 (green points).

Preprints (www.preprints.org) | NOT PEER-REVIEWED | Posted: 19 February 2021 doi:10.20944/preprints202102.0427.v1

This behavior can be interpreted in the light of the information collected in a previous contribution [10] about the state of water molecules, at equilibrium, within the PEI/water mixture as a function of their concentration. In fact, at low concentration, water molecules are prevalently present as *first shell* water. *First shell* water is mainly contributed by molecules bridging, by hydrogen bonds, two consecutive carbonyl groups present along a macromolecule and, at a lesser extent, by molecules bridging, by hydrogen bonds, two non-consecutive carbonyls located on two different macromolecules or to different repeating units of the same macromolecule. Conversely, as the water concentration increases, the concentration of so-called *second shell water* molecules increases. *Second shell water* refers to those water molecules that interact, by a single hydrogen bond, with a *first shell water* molecule. Due to the structure of the interaction complex, *first shell* water is characterized by a stronger energy of interaction with the PEI carbonyls as compared with the energy of interaction of *second shell* water molecules with a *first shell* water molecule.

It is then expected that at low water concentration a lower mobility (diffusivity) should be observed and that mobility should increase with concentration, in agreement with reported results of MD simulations. In order to deepen understanding of this effect, water molecules have been grouped in sets according to their diffusion coefficient and the fraction of the simulation time spent in the first shell state has been calculated averaging over each molecule set. The results of this analysis are reported in Figure 7C. From this figure it is clear that sets of water molecules spending a large fraction of simulation time in the *first shell* bridging state are characterized by a lower mobility. On the contrary, larger diffusion coefficients are obtained for sets of water molecules spending most of the simulation time in states different from *first shell*.

4.3. Comparison of theoretical predictions with results of vibrational spectroscopy

In figure 8 is reported the comparison between the values of the *mutual-diffusion* coefficient, D_{12}, determined experimentally by FTIR spectroscopy and discussed in section 4.1, and the values of this coefficient predicted using in equation (15b) the values of D_1 estimated by MD calculations and the values of $\left(\frac{\partial \mu_1}{\partial \ln x_1}\right)_{T,P}$ estimated using the NETGP-NRHB model. In order to compare experimental results with theoretical findings, values of mutual diffusivity estimated from the experimental differential sorption steps by fitting sorption kinetics using eq. (16) are reported as a

Preprints (www.preprints.org) | NOT PEER-REVIEWED | Posted: 19 February 2021 doi:10.20944/preprints202102.0427.v1

function of the average water mass fraction present within the polymer during the test, calculated as the arithmetic average of the uniform initial and final water mass fraction.

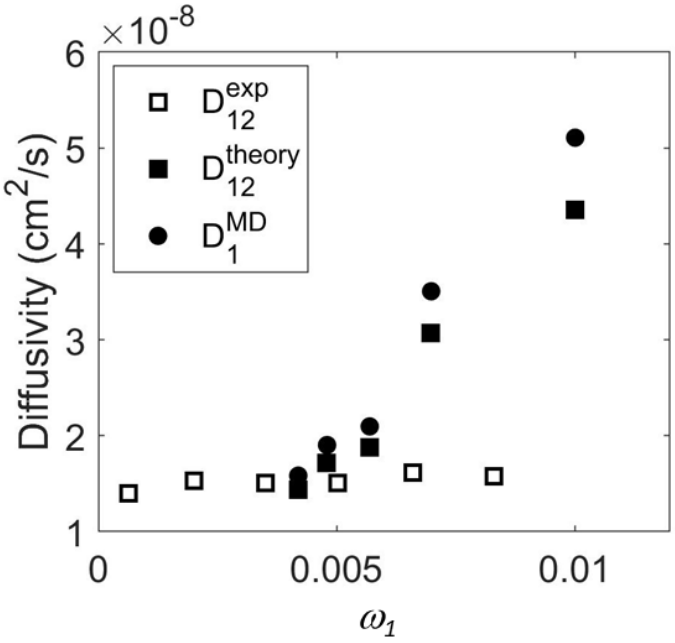

Figure 8. Values of water *intra-diffusion* coefficient determined from MD simulations, D_1^{MD}, of water-PEI mutual diffusion coefficient determined from eq. (15b), D_{12}^{theory}, and of water-PEI mutual diffusion coefficient determined experimentally from FTIR spectroscopy, D_{12}^{exp}.

As already discussed in section 4.1, the experimental results obtained by FTIR spectroscopy point out that, in the whole range investigated, the *mutual diffusion* coefficient is roughly constant as a function of penetrant concentration. The theoretical values of D_{12} seemingly approach the experimental values when water concentration tends to zero. We remind that, in this limit, the theoretical values of D_{12} and D_1 tend to the same value. Conversely, as the concentration increases, a gradually increasing departure of the theoretical values of D_{12} from the experimental values is evident. This mismatch could be attributed to the fact that, as reported in literature [35], the MD approach implemented here is reliable at quite low penetrant concentration while it provides a progressively increasing overestimation of the dependence of *intra-diffusion* coefficient as the water concentration increases and, in turn, an increasing overestimation of D_{12} values.

4.4 H-bond lifetimes

Preprints (www.preprints.org) | NOT PEER-REVIEWED | Posted: 19 February 2021 doi:10.20944/preprints202102.0427.v1

An interesting additional information that can be obtained from MD simulations is the time-dependent behavior of the H-bonds, the most accessible property reflecting this kind of behavior being the mean bond lifetime.

In order to estimate H-bond lifetimes, we extracted from the simulation data the time-dependent autocorrelation functions of state variables which reflect the existence (or non-existence) of bonds between each of the possible donor acceptor pairs. According with references [36] [37] [38-40] the HB correlation function *C*(*t*) is defined as following:

$$C(t) = \sum_{ij} s_{ij}(t_0)s_{ij}(t_0 + t) / \sum_{ij} s_{ij}(t_0) \qquad (17)$$

where the dynamical variable $s_{ij}(t)$ equals unity if the particular tagged pair of molecules is hydrogen bonded and is zero otherwise. The sums are over all pairs and t_0 is the time at which the measurement period starts (C*(0)* =1).

The H-bond life time, τ, is readily defined from the exponential decay of *C(t):*

$$C(t) = A\exp(-t/\tau) \qquad (18)$$

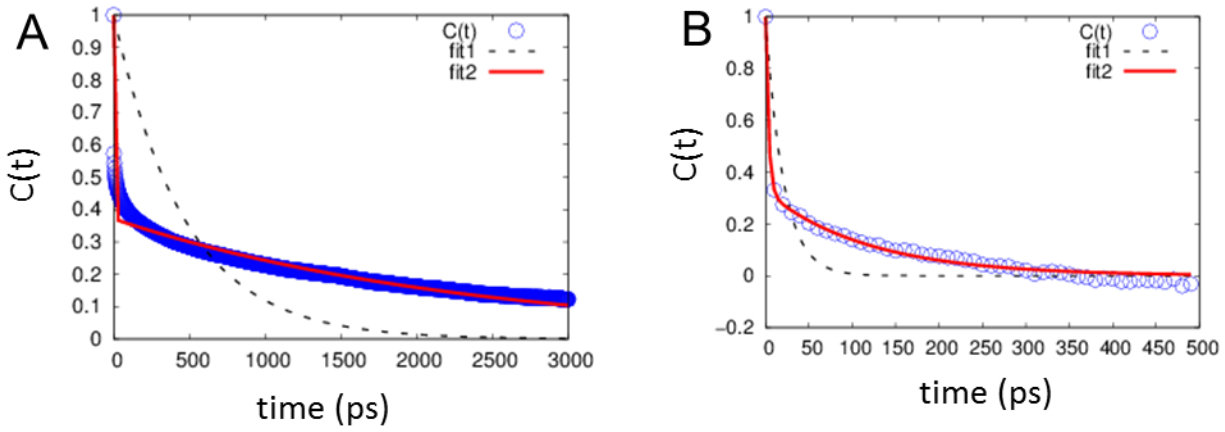

Figure 9. Time behavior of continuous HB correlation functions for System II (A) and System VII (**B**)

In our analysis *C(t)* of H-bond functions has been calculated as continuous hydrogen bond correlation functions, meaning that each s_{ij} variable is allowed to make just one transition from unity to zero when the H-bond is first observed to break, but is not allowed to return to unity should the

Preprints (www.preprints.org) | NOT PEER-REVIEWED | Posted: 19 February 2021 doi:10.20944/preprints202102.0427.v1

same bond reform subsequently. On the base of the results reported in [10], we confined our analysis to one kind of HB acceptor that is the carboxylic group (defined as AC1 in [10]). In Fig. 9 *C(t)* corresponding to system II (the one containing 86 water molecules) and system VII (the one containing 220 water molecules) are reported. Interestingly, no reasonable fitting of *C(t)* correlation functions was obtained using a single exponential decay (see dashed lines in both figures). Instead, a better agreement has been obtained using a sum of two different exponential decays, i.e.:

$$C(t) = A_1 \exp(-t/\tau_1) + A_2 \exp(-t/\tau_2) \quad (19)$$

Table 2. HB Life time values and relative population weights (A_1 and A_2) obtained fitting the HB autcorrelation functions by eq. (17)

System	τ_1	τ_2	A_1	A_2
II	4.4 ps	2362 ps	0.62	0.38
VI	3.9 ps	118 ps	0.67	0.33

We identify a fast decay of about 4 ps and a slower one going from about 2 ns for the system at low water concentration to 118 ps for the system at higher water content, see table 2. A similar range of lifetimes has been reported in other simulation analyses, indicating also values in excess of 1 ns for interacting glassy polymers. [41] Moreover, this feature is in agreement with the identification of two water populations: one consisting in water molecule bridging two carbonyls of PEI (slower decay) and one consisting of water molecules interacting with *first shell* water molecules (faster decay). In [10], as already recalled in sections 4.1 and 4.2, we have also demonstrated that two types of *first shell* bridging HB can exist: intrachain and interchain first shell HB, depending on if the two carbonyls are consecutive on the same chain or belonging to separate chains.

Interchain water bridges are present at lower extent going from a fraction of 0, at the lowest water concentration (system II), to a fraction around 0.3, of all bridged molecules, at higher water concentration (system VII). Structural analysis clearly shows that in the case of *first shell* intrachain HB the distances between the carbonyl oxygens and water's oxygens are shored and their distribution are narrow, compared to those of *first shell* interchain hydrogen bonded water molecules, indicating an higher mobility of the latter with respect to the former ones. So the

Preprints (www.preprints.org) | NOT PEER-REVIEWED | Posted: 19 February 2021 doi:10.20944/preprints202102.0427.v1

increase of interchain first shell HB in higher water concentration system further contributes to decrease H-bond life time for first shell HB population.

As final remark, it is worth noticing that lifetimes of the order of several picoseconds for the second-shell water molecules are consistent with the experimental observation of two distinct signals generated by this species in the vibrational spectrum. In fact, since the characteristic decay time of vibrational transitions is of the order of a picosecond, shorter H-bonding lifetimes would produce a fully convoluted bandshape rather than the well-resolved profile that is observed.

CONCLUSIONS

The diffusion of water in PEI as determined experimentally by time-resolved FTIR spectroscopy has been interpreted on the basis of MD simulations combined with modeling of water chemical potentials by means of a non-equilibrium lattice fluid model for thermodynamics of water/PEI system. Based on the physical picture on H-bonding formation obtained in a previous investigation, the diffusion process has been investigated by MD simulations of systems with different compositions. The results of the theoretical analysis are quantitatively consistent with the experimental results provided by FTIR spectroscopy, in terms of mutual diffusion coefficient, in the limit of vanishingly small water concentration. However, the predictions obtained from the theoretical analysis provide values of mutual diffusivity that increasingly depart from the experimentally determined values, as concentration of water increases, likely due to limitations of MD simulation approach. Based on the analysis of trajectories of diffusing water molecules resulting from MD, it has also been elucidated the role played by the different types of self- and cross-HB established in the system in determining the value of mutual binary diffusion coefficient. The analysis evolution of H-bond lifetimes as it emerges from MD, provides a convincing qualitative picture of the diffusion process of water molecules in the PEI matrix.

ACKNOWLEDGE

The authors gratefully acknowledge Prof. Giuseppe Milano for the useful discussions and suggestions which significantly helped us in our investigation.

References

1. Mensitieri, G.; Iannone, M., *Ageing of Composites*, 2008.
2. Li, D.; Yao, J.; Wang, H.; Hoek, E. M. V.; Tarabara, V. V., *Encyclopedia of Membrane Science and Technology*, 2013.
3. Bernstein, R.; Kaufman, Y.; Freger, V.; Hoek, E. M. V.; Tarabara, V. V., *Encyclopedia of Membrane Science and Technology*, 2013.
4. Brunetti, A.; Barbieri, G.; Drioli, E.; Hoek, E. M. V.; Tarabara, V. V., *Encyclopedia of Membrane Science and Technology*, 2013.
5. Koros, W. J.; Fleming, G. K.; Jordan, S. M.; Kim, T. H.; Hoehn, H. H., Polymeric Membrane Materials for Solution-Diffusion Based Permeation Separations. *Prog. Polym. Sci.* **1988**, *13*, 339.
6. Christie, S.; Scorsone, E.; Persaud, K.; Kvasnik, F., Remote Detection of Gaseous Ammonia Using the near Infrared Transmission Properties of Polyaniline. *Sens. Actuators, B* **2003**, *90*, 163.
7. Scherillo, G.; Petretta, M.; Galizia, M.; La Manna, P.; Musto, P.; Mensitieri, G., Thermodynamics of Water Sorption in High Performance Glassy Thermoplastic Polymers. *Front. Chem.* **2014**, *2*, 25.

8. Scherillo, G.; Galizia, M.; Musto, P.; Mensitieri, G., Water Sorption Thermodynamics in Glassy and Rubbery Polymers: Modeling the Interactional Issues Emerging from Ftir Spectroscopy. *Ind. Eng. Chem. Res.* **2013**, *52*, 8674.
9. Scherillo, G.; Sanguigno, L.; Galizia, M.; Lavorgna, M.; Musto, P.; Mensitieri, G., Non-Equilibrium Compressible Lattice Theories Accounting for Hydrogen Bonding Interactions: Modelling Water Sorption Thermodynamics in Fluorinated Polyimides. *Fluid Phase Equilib.* **2012**, *334*, 166.
10. De Nicola, A.; Correa, A.; Milano, G.; La Manna, P.; Musto, P.; Mensitieri, G.; Scherillo, G., Local Structure and Dynamics of Water Absorbed in Poly(Ether Imide): A Hydrogen Bonding Anatomy. *The Journal of Physical Chemistry B* **2017**, *121*, 3162-3176.
11. Mensitieri, G.; Scherillo, G.; Panayiotou, C.; Musto, P., Towards a Predictive Thermodynamic Description of Sorption Processes in Polymers: The Synergy between Theoretical Eos Models and Vibrational Spectroscopy. *Materials Science and Engineering: R: Reports* **2020**, *140*, 100525.
12. Panayiotou, C.; Pantoula, M.; Stefanis, E.; Tsivintzelis, I.; Economou, I. G., Nonrandom Hydrogen-Bonding Model of Fluids and Their Mixtures. 1. Pure Fluids. *Ind. Eng. Chem. Res.* **2004**, *43*, 6592.
13. Panayiotou, C.; Tsivintzelis, I.; Economou, I. G., Nonrandom Hydrogen-Bonding Model of Fluids and Their Mixtures. 2. Multicomponent Mixtures. *Ind. Eng. Chem. Res.* **2007**, *46*, 2628.
14. Bird, R. B. S., W.E.; Lightfoot, E.N. , *Transport Phenomena* John Wiley & Sons: New York, 2007.
15. Crank, J., *The Mathematics of Diffusion*; Claredon Press: Oxford, 1975.
16. Bearman, R. J., On the Molecular Basis of Some Current Theories of Diffusion1. *The Journal of Physical Chemistry* **1961**, *65*, 1961-1968.
17. Caruthers, J. In *Handbook of Diffusion and Thermal Properties of Polymers and Polymer Solutions*, 1998.
18. Vrentas, J. S.; Duda, J. L., Diffusion in Polymer–Solvent Systems. Ii. A Predictive Theory for the Dependence of Diffusion Coefficients on Temperature, Concentration, and Molecular Weight. *J. Polym. Sci., Polym. Phys. Ed.* **1977**, *15*, 417.
19. Vrentas, J. S.; Vrentas, C. M., Predictive Methods for Self-Diffusion and Mutual Diffusion Coefficients in Polymer–Solvent Systems. *Eur. Polym. J.* **1998**, *34*, 797.
20. Cotugno, S.; Larobina, D.; Mensitieri, G.; Musto, P.; Ragosta, G., A Novel Spectroscopic Approach to Investigate Transport Processes in Polymers: The Case of Water–Epoxy System. *Polymer* **2001**, *42*, 6431.
21. Jorgensen, W. L.; Nguyen, T. B., Monte Carlo Simulations of the Hydration of Substituted Benzenes with Opls Potential Functions. *J. Comput. Chem.* **1993**, *14*, 195.
22. Jorgensen, W. L.; Maxwell, D. S.; TiradoRives, J., Development and Testing of the Opls All-Atom Force Field on Conformational Energetics and Properties of Organic Liquids. *J. Am. Chem. Soc.* **1996**, *118*, 11225.
23. Price, M. L. P.; Ostrovsky, D.; Jorgensen, W. L., Gas-Phase and Liquid-State Properties of Esters, Nitriles, and Nitro Compounds with the Opls-Aa Force Field. *J. Comput. Chem.* **2001**, *22*, 1340.
24. Milano, G.; Muller-Plathe, F., Cyclohexane;Benzene Mixtures:Thermodynamics and Structure from Atomistic Simulations. *J. Phys. Chem. B* **2004**, *108*, 7415.
25. Tironi, I. G.; Sperb, R.; Smith, P. E.; van Gunsteren, W. F., A Generalized Reaction Field Method for Molecular Dynamics Simulations. *J. Chem. Phys.* **1995**, *102*, 5451.

26. Berendsen, H. J. C.; Postma, J. P. M.; van Gunsteren, W. F.; Hermans, J.; Pullman, B., *Intermolecular Forces: Proceedings of the Fourteenth Jerusalem Symposium on Quantum Chemistry and Biochemistry Held in Jerusalem, Israel, April 13–16, 1981*, 1981, p 331.
27. Milano, G.; Kawakatsu, T., Hybrid Particle-Field Molecular Dynamics Simulations for Dense Polymer Systems. *J. Chem. Phys.* **2009**, *130*, 214106.
28. Milano, G.; Kawakatsu, T., Pressure Calculation in Hybrid Particle-Field Simulations. *J. Chem. Phys.* **2010**, *133*, 214102.
29. Zhao, Y.; De Nicola, A.; Kawakatsu, T.; Milano, G., Hybrid Particle-Field Molecular Dynamics Simulations: Parallelization and Benchmarks. *J. Comput. Chem.* **2012**, *33*, 868.
30. De Nicola, A.; Kawakatsu, T.; Milano, G., Generation of Well-Relaxed All-Atom Models of Large Molecular Weight Polymer Melts: A Hybrid Particle-Continuum Approach Based on Particle-Field Molecular Dynamics Simulations. *J. Chem. Theory Comput.* **2014**, *10*, 5651.
31. Van der Spoel, D.; Lindahl, E.; Hess, B.; Groenhof, G.; Mark, A. E.; Berendsen, H. J. C., Gromacs: Fast, Flexible, and Free. *J. Comput. Chem.* **2005**, *26*, 1701.
32. Berendsen, H. J. C.; Postma, J. P. M.; Gunsteren, W. F. v.; DiNola, A.; Haak, J. R., Molecular Dynamics with Coupling to an External Bath. *J. Chem. Phys.* **1984**, *81*, 3684.
33. Musto, P.; La Manna, P.; Cimino, F.; Mensitieri, G.; Russo, P., Morphology, Molecular Interactions and H(2)O Diffusion in a Poly(Lactic-Acid)/Graphene Composite: A Vibrational Spectroscopy Study.
34. Musto, P.; Ragosta, G.; Mensitieri, G.; Lavorgna, M., On the Molecular Mechanism of H2o Diffusion into Polyimides: A Vibrational Spectroscopy Investigation. *Macromolecules* **2007**, *40*, 9614.
35. Milano, G.; Guerra, G.; Müller-Plathe, F., Anisotropic Diffusion of Small Penetrants in the Δ Crystalline Phase of Syndiotactic Polystyrene: A Molecular Dynamics Simulation Study. *Chemistry of Materials* **2002**, *14*, 2977-2982.
36. Rapaport, D. C., Hydrogen Bonds in Water. *Molecular Physics* **1983**, *50*, 1151-1162.
37. Chowdhuri, S.; Chandra, A., Dynamics of Halide Ion−Water Hydrogen Bonds in Aqueous Solutions: Dependence on Ion Size and Temperature. *The Journal of Physical Chemistry B* **2006**, *110*, 9674-9680.
38. Luzar, A., Resolving the Hydrogen Bond Dynamics Conundrum. *J. Chem. Phys.* **2000**, *113*, 10663.
39. Luzar, A.; Chandler, D., Hydrogen-Bond Kinetics in Liquid Water. *Nature* **1996**, *379*, 55-57.
40. Luzar, A.; Chandler, D., Effect of Environment on Hydrogen Bond Dynamics in Liquid Water. *Physical Review Letters* **1996**, *76*, 928-931.
41. Mijović, J.; Zhang, H., Molecular Dynamics Simulation Study of Motions and Interactions of Water in a Polymer Network. *J. Phys. Chem. B* **2004**, *108*, 2557.